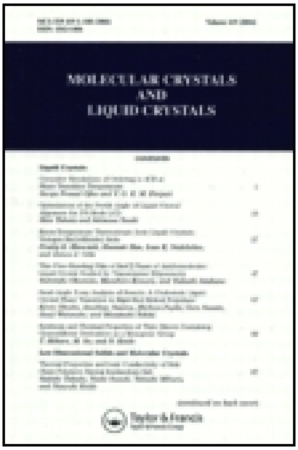

Molecular Crystals and Liquid Crystals
Publication details, including instructions for authors and subscription information:
http://www.tandfonline.com/loi/gmcl20

NUMERICAL STUDY OF A LENS-SHAPED LIQUID CRYSTAL CELL

Bin Wang [a] , Mao Ye [a] & Susumu Sato [a]
[a] Department of Electrical and Electronic Engineering, Akita University, 1-1 Tegatagakuen-cho 010-8502 Akita, Japan

Version of record first published: 07 Jan 2010

To cite this article: Bin Wang, Mao Ye & Susumu Sato (2004): NUMERICAL STUDY OF A LENS-SHAPED LIQUID CRYSTAL CELL, Molecular Crystals and Liquid Crystals, 413:1, 423-433

To link to this article: http://dx.doi.org/10.1080/15421400490438979

Mol. Cryst. Liq. Cryst., Vol. 413, pp. 423/[2559]–433/[2569], 2004

ISSN: 1542-1406 print/1563-5287 online
DOI: 10.1080/15421400490438979

NUMERICAL STUDY OF A LENS-SHAPED LIQUID CRYSTAL CELL

Bin Wang, Mao Ye, and Susumu Sato
Department of Electrical and Electronic Engineering, Akita University, 1-1 Tegatagakuen-cho, 010-8502 Akita, Japan

Molecular orientation properties of a lens-shaped liquid crystal cell are studied numerically. The cell is found to have a good optical quality as a lens and its focal length changes with the applied voltage in the case that the applied voltage is increased gradually. On the other hand, if a high voltage is applied directly, disclination lines may appear.

Keywords: difference equation; disclination line; liquid crystal lens; phase retardation; spherical boundary

INTRODUCTION

With proper electric electrode structures, bell-like refractive index distributions can be formed in liquid crystal (LC) cells by non-uniform electric fields, and the LC cells behave like optical lenses. The focus of an LC lens can be changed by an applied voltage. Several LC lenses have been reported. A LC microlens [1] has good optical properties, but its size is generally limited at around several hundred micrometers. Lenses of larger size were obtained by using an electrode with a distributed reactive electrical impedance [2], or an insulating layer between the LC and the electrode [3]. Since thin layers of LCs are used in these LC lenses, the phase retardations of incident light beams are small, for they are induced by the refractive index variances, and hence the numerical apertures are small.

The LC lens fabricated by filling an LC into a lens-shaped LC cell [4] has large numerical aperture, for the phase retardation is resulted from both the refractive index and the thickness differences. Furthermore, the optical quality of the lens is rather good. However, there still lack an understanding of the complicated interaction between the electric field and the directors,

Address correspondence to Bin Wang, Department of Electrical and Electronic Engineering, Akita University, 1-1 Tegatagakuen-cho, 010-8502 Akita, Japan.

which is essential to design LC lenses of high optical quality. In this paper, we give a numerical study on the LC cell. The reorientation of the directors and the phase profiles of an incident light beam are obtained. Some physical discussions are presented. A mathematical technology to handle the spherical boundary in a Cartesian coordinate is developed, which we believe can be widely applied to other calculations with regard to irregular boundary conditions.

METHOD

The typical structure of a lens-shaped LC cell is shown in Figure 1. A plano-concave glass lens is placed on a plane glass substrate to form a lens-shaped chamber, into which a nematic LC is filled. Here, the LC directors are homogenous alignment at both the surfaces of the glass lens and the plane glass substrates.

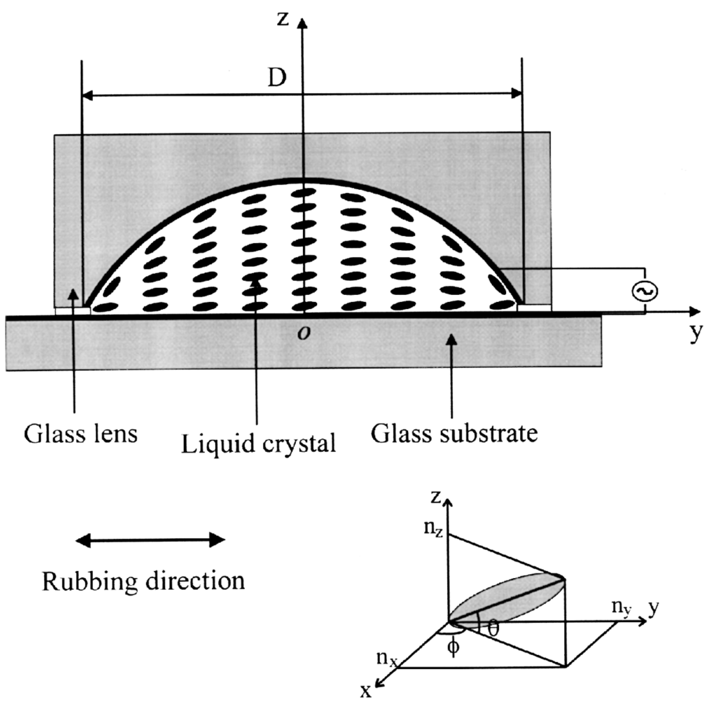

FIGURE 1 Structure of lens-shaped LC cell.

The orientation of the LC directors satisfies the equation

$$-\frac{\partial f}{\partial u}+\frac{\partial}{\partial \beta}\left[\frac{\partial f}{\partial\left(\frac{\partial u}{\partial \beta}\right)}\right]=0, \tag{1}$$

where u denotes n_x, n_y, n_z, or the applied voltage V, and β x, y, or z. The free energy density [5]

$$f=\frac{1}{2}\left[K_{11}(\nabla\cdot\boldsymbol{n})^2+K_{22}(\boldsymbol{n}\cdot\nabla\times\boldsymbol{n})^2+K_{33}(\boldsymbol{n}\times\nabla\times\boldsymbol{n})^2\right]-\frac{1}{8\pi}(\varepsilon\cdot\boldsymbol{E})\cdot\boldsymbol{E}, \tag{2}$$

where K_{11}, K_{22} and K_{33} are the splay, twist and bend elastic constants, respectively, ε the dielectric constant of the LC, and $\boldsymbol{E}$ the intensity of the electric field. The director vector

$$\boldsymbol{n}=(n_x,n_y,n_z)=(\cos\theta\cos\phi,\ \cos\theta\sin\phi,\ \sin\theta), \tag{3}$$

where θ is the tilt angle and ϕ the azimuthal one (Fig.1). Strong anchoring at both surfaces of the glass lens and the plane substrate are assumed.

Putting $\boldsymbol{E}=(-dV/dx,-dV/dy,-dV/dz)$ into Eq. (2) and substituting Eqs. (2) and (3) into Eq. (1), the nonlinear differential equations for n_x, n_y, n_z and V are obtained. To solve the equations, a spherical coordinate system seems to be convenient in account of the calculation with the spherical boundary condition, but when θ approaches to $\pi/2$, the derivatives of ϕ become infinite [6,7]. So a Cartesian coordinate system is used. In a Cartesian coordinate system, the spherical boundary locates usually at positions between two mesh points. The treatment for 'extraordinary' mesh points, that is, the points 'near' the boundary (P_1 and P_2, for example, in Fig. 2.), is different from that for the ordinary points, that is, the points 'far from' the boundary (P, for example, in Fig. 2.). Let us take the second-order derivatives of $u(x,y,z)$ at P_1, P_2 and P with respect to x as examples.

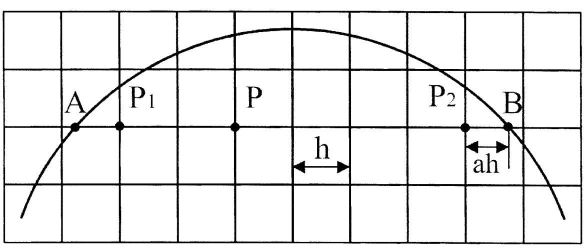

FIGURE 2 Spherical boundary.

The difference equations are [8]

$$\frac{\partial^2 u(x,y,z)}{\partial x^2} = \frac{2}{h^2}\left\{\frac{u_A}{a(x,y,z)[a(x,y,z)+1]} + \frac{u(x+h,y,z)}{a(x,y,z)+1} - \frac{u(x,y,z)}{a(x,y,z)}\right\} \tag{4}$$

at P_1,

$$\frac{\partial^2 u(x,y,z)}{\partial x^2} = \frac{2}{h^2}\left\{\frac{u_B}{a(x,y,z)[a(x,y,z)+1]} + \frac{u(x-h,y,z)}{a(x,y,z)+1} - \frac{u(x,y,z)}{a(x,y,z)}\right\} \tag{5}$$

at P_2, and

$$\frac{\partial^2 u(x,y,z)}{\partial x^2} = \frac{2}{h^2}\left\{\frac{u(x+h,y,z)}{2} + \frac{u(x-h,y,z)}{2} - u(x,y,z)\right\} \tag{6}$$

at P, where h is the step size and $a(x,y,z)$ is defined below. In the difference equation at an ordinary point P, the quantity at the left point $u(x-h,y,z)$ and that at the right point $u(x+h,y,z)$ are symmetrical. In the equations at extraordinary points, however, they are not. It is difficult for program to treat the differene equations for $u(x,y,z)$ at P_1 and P_2 automatically. The workflow in our calculation is: (1) For x $\geq$ 0, calculate the distance d of a mesh point from the right boundary, and for x $<$ 0, that from the left boundary. If $d \geq h$, then the point is an ordinary point. If $d < h$, then it is an extraordinary point. (2) Define a parameter $a(x,y,z)$ for each mesh point P_i. For an ordinary point, $a(x,y,z) = 1$; for an extraordinary one $a(x,y,z) = d/h$. (3) For x $\geq$ 0 ,the quantity at each point P_i is divided by the paramter $a(x,y,z)$ associated with the left point, that is, $u(x+h,y,z) = u(x+h,y,z)/a(x,y,z)$, and for x $<$ 0, the quantity at each point P_i is divided by the parameter $a(x,y,z)$ associated with the right point, that is, $u'(x-h,y,z) = u(x-h,y,z)/a(x,y,z)$. Then the values of $u(x,y,z)$ at the boundary are modified to be $u'_A = u_A/a(x,y,z)$ and $u'_B = u_B/a(x,y,z)$, while the values of $u(x,y,z)$ at points in the cell remain unchanged. (4) Modify the difference equations for extraordinary points as

$$\frac{\partial^2 u(x,y,z)}{\partial x^2} = \frac{2}{h^2}\left[\frac{u'_A}{a(x,y,z)+1} + \frac{u(x+h,y,z)}{a(x,y,z)+1} - \frac{u(x,y,z)}{a(x,y,z)}\right] \tag{7}$$

at P_1 and

$$\frac{\partial^2 u(x,y,z)}{\partial x^2} = \frac{2}{h^2}\left[\frac{u'_B}{a(x,y,z)+1} + \frac{u(x-h,y,z)}{a(x,y,z)+1} - \frac{u(x,y,z)}{a(x,y,z)}\right] \tag{8}$$

TABLE 1 Quantities Used in the Calculation

Quantity	R (mm)	D (mm)	K_{11} (μdyne)	K_{22} (μdyne)	K_{33} (μdyne)	$\varepsilon_{\perp}$
Value	51.90	10	10.2	6.4	15.5	3.6
Quantity	$\varepsilon_{//}$	n_e	n_o	n_g	λ (μm)	θ (deg)
Value	6.3	1.766	1.524	1.457	0.633	2

at P_2. Then for extraordinary points, th quantities at the left and right points in the difference equations also appear symmetrical. The treatments for all points in the cell become the same.

The equations for n_x, n_y, n_z, and V are solved with a relaxation method. At each loop, $\boldsymbol{n}$ is normalized to maintain $|\boldsymbol{n}| = 1$. With known $\boldsymbol{n}$, the effective refractive index seen by a normally incident light beam linearly polarized in the rubbing direction is

$$n_e(\theta) = \frac{n_o n_e}{(n_e^2 \sin^2\theta + n_0^2 \cos^2\theta)^{1/2}}, \tag{5}$$

where n_o and n_e are, respectively, the ordinary and the extraordinary refractive indices of the liquid crystal. The induced phase retardation of the light beam is then

$$\varphi = \frac{2\pi}{\lambda}\int_0^d [n_e(\theta) - n_g]dz, \tag{6}$$

where d is the maximum thickness of the LC layer, n_g the refractive index of the glass, and λ the wavelength of the light beam.

Quantities used in the calculation are list in Table 1, where R is the radius of curvature, $\varepsilon_{\|}$ and $\varepsilon_{\perp}$ the dielectric constants parallel and perpendicular to the local director, respectively, and θ_0 the pre-tilt angle of directors at the surface of the substrates. The voltage applied on the cell is normalized by $V_c = 2\pi(\pi K_{11}/\Delta\varepsilon)^{1/2}$.

RESULTS AND DISCUSSION

The initial orientation of the directors in the plane of x = 0 when $V = 0$ is shown in Figure 3(a). The short bars represent the directors. The directors at the surfaces of the spherical lens substrate are not included in the figure. The horizontal bars in the region outside the LC cell have no meanings. The

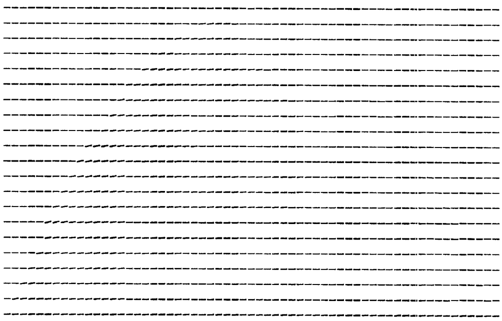

(a)

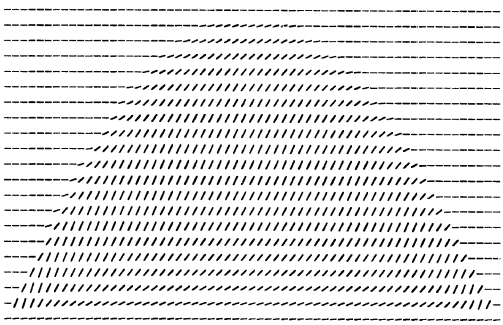

(b)

FIGURE 3 Directors in the plane of x = 0. (a) V = 0. (b) V = 1.3.

orientations of the directors are governed by the elastic force exerted by the surfaces of the LC cell. For the directors at the surfaces of both the glass lens and plane glass substrates have a pretilt angle θ_0, there are small tilt angles for the directors in the LC cell.

When a voltage is applied, the directors are acted jointly by the elastic and the electric forces. The tilt angle θ increases, at a voltage $V = 1.3$, the director orientation is shown in Figure 3(b). As θ increases, the incident light beam sees a smaller refractive index, and experiences a smaller phase retardation φ. Figure 4 shows φs at voltages 0, 1.1 and 1.3. The upper plots are the three-dimensional distributions of φs and lower ones are φs along the rubbing direction and the direction perpendicular to the rubbing direction. The curves in the lower plots represent the quadratic fittings. It can be seen that φ decreases with the voltage. There is a difference between φ along the rubbing direction and along the perpen-

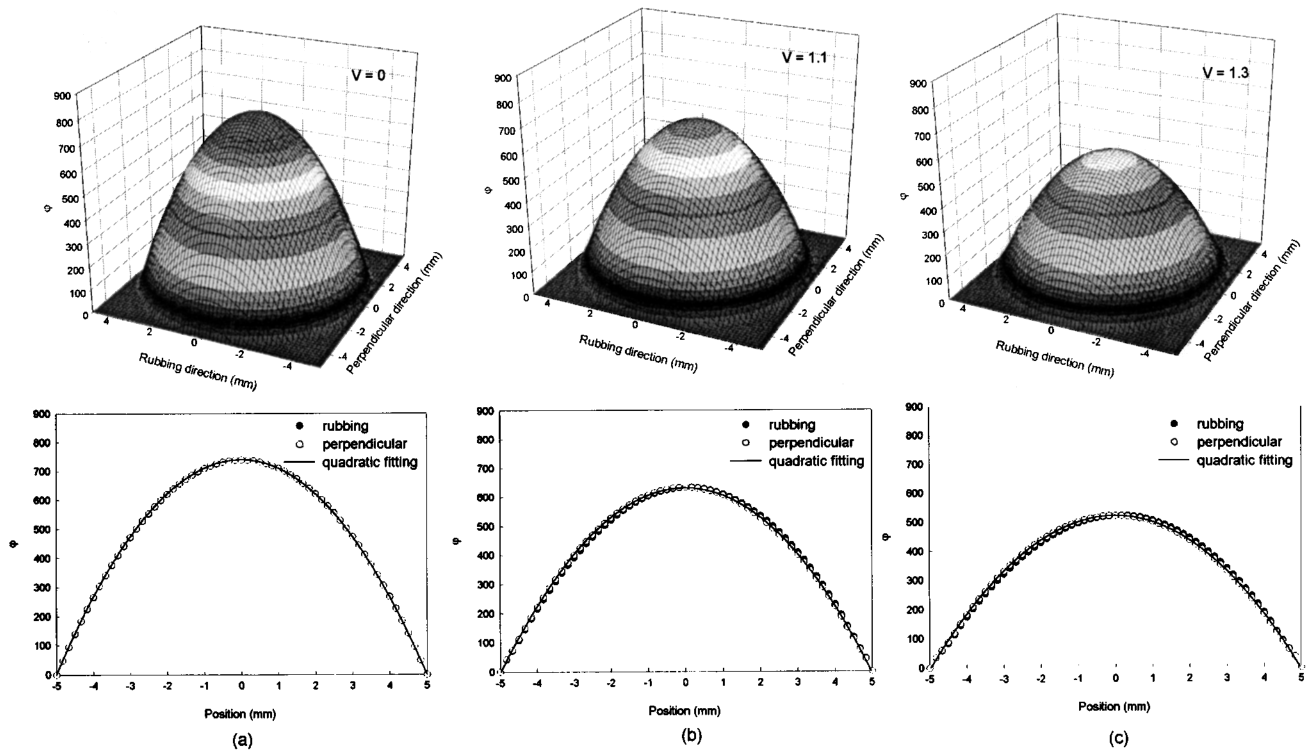

FIGURE 4 Phase retardations. (a) V = 0. (b) V = 1.1. (c) V = 1.3.

dicular direction due to the anisotropy of the directors, but it is very small, and the profiles of φs are nearly quadratic at various voltages. So the cell exhibits a good lens property and the phase retardation experienced by the incident light beam is a function of the applied voltage.

As φ changes with V, the focal length f of the LC cell is also a function of the applied voltage. Figure 5 shows how f changes with V. As V approaches to V_c, f begins to increase. When V is high enough, θs of most directors in the LC cell approach to $\pi/2$ and f stops increasing with V. It is interesting to note that there is a remarkable reorientation of directors in the LC cell only when V approaches to V_c. V_c is the voltage applied to a cell with planar substrates, at which the Fredericksz transition takes place. In the case of the LC lens, V_c loses its physical meaning and is only used as a convenient quantity to scale voltage in the calculation. But it seems that only after V exceeds V_c, directors in the LC cell as a whole begins to rotate. The result is understandable if we note that the curvature of the sphere is very large, and some of the properties of the cell are very similar to the cell with plane substrates.

In the above calculation, we increase the voltage gradually from 0 to a specific value. If the voltage is applied directly from 0 to a high value, the orientation of directors in the cell may take a different form. Figure 6(a) shows the directors in the plane of x = 0, in the case that V is applied

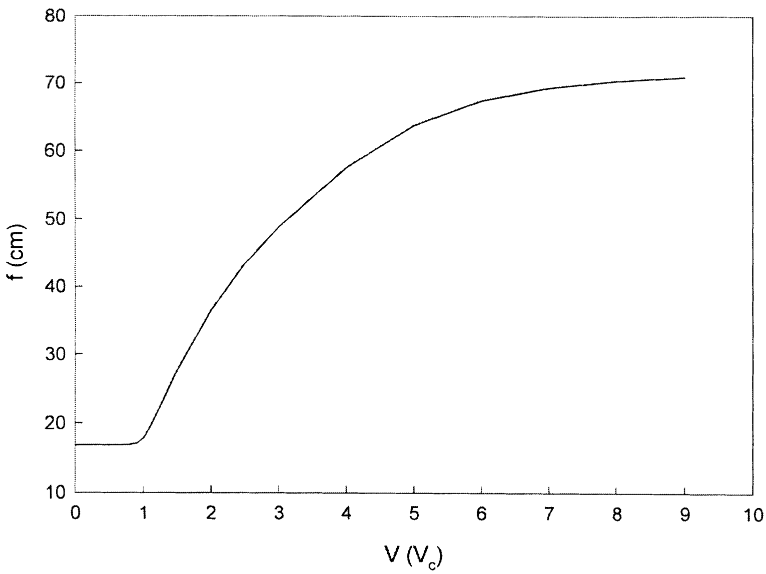

FIGURE 5 Focal length vs voltage.

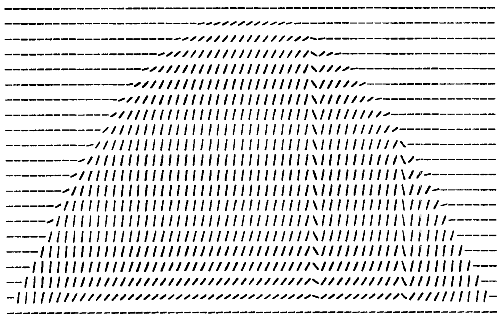

(a)

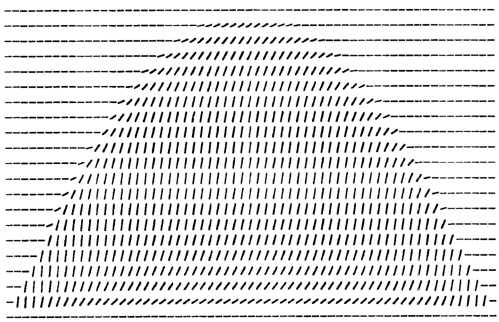

(b)

FIGURE 6 Directors at V = 1.9 in the plane of x = 0. (a) V = 1.9 applied directly. (b) V = 1.9 applied gradually.

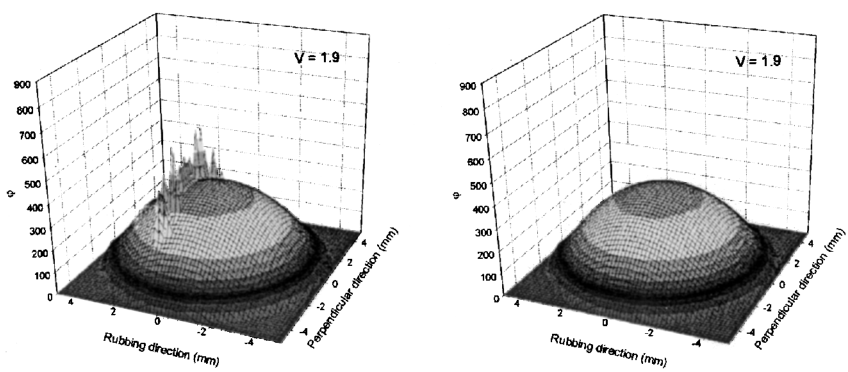

(a) (b)

FIGURE 7 Phase retardations at V = 1.9. (a) V = 1.9 applied directly. (b) V = 1.9 applied gradually.

directly from 0 to 1.9. It can be seen that the LC cell is divided into domains of the different rotating directions. In neighboring domains directors rotate in opposite directions. The rotations of directors are governed by the elastic force exerted by the surfaces and the electric field. The direction of the electric field differs with position and so is that of the directors. The angle between the directors and the electric field also differs with position. When V is high enough, electric force dominates, and the directors in different regions in the cell may rotate in different directions, and disclination lines may appear. On the other hand, if the voltage is increases gradually, the directors rotate gradually with the applied voltage in the direction of the pretilt angle, and most of the directors finally orientate in the same direction, and no disclination lines occur. Figure 6(b) shows the directors in the plane of $x = 0$, when V is gradually increased from 0 to 1.9. In the case of direct application of high voltage, there are abrupt changes in φ, as shown in Figure 7(a). On the other hand, gradual application of high voltage results in a smooth phase retardation, as shown in Figure 7(b). The phenomena are also observed in previous experiments [4,9].

CONCLUSIONS

A numerical study on the lens-shaped LC cell is presented. The director reorientations and the phase retardation of an incident light beam are given by the simulation. It is shown that the LC cell has a good optical property in the case that the applied voltage is increased gradually, and the focal length of the cell is a function of the applied voltage. The simulation reveals the mechanism of the interaction between the electric field and the directors. Some experimental phenomena such as the occurring of the disclination lines are understood by this study. This work is very useful in design of the lens-shaped LC cell of high optical quality.

REFERENCES

[1] Nose, T. & Sato, S. (1989). A liquid crystal microlens obtained with a non-uniform electric field. *Liq. Cryst.*, *5*, 1425–1433.
[2] Naumov, A. F., Loktev, M. Yu., Guralnik, I. R., & Vdovin, G. (1998). Liquid-crystal adaptive lenses with modal control. *Opt. Lett.*, *23*, 992–994.
[3] Ye, M. & Sato, S. (2002). Optical properties of liquid crystal lens of any size. *Jpn. J. Appl. Phys.*, *41*, L571–L573.
[4] Sato, S. (1979). Liquid-crystal lens-cells with variable focal length. *Jpn. J. Appl. Phys.*, *18*, 1679–1684.
[5] de Gennes, P. G. (1974). *The Physics of Liquid Crystal*. Oxford University Press: London.
[6] van Doorn, C. Z. (1975). Dynamic behavior of twisted nematic liquid-crystal layers in switched fields. *J. Appl. Phys.*, *46*, 3738–3745.

[7] Mori, H., Gartland, E. C., Jr., Kelly, J. R., & Bos, P. J. (1999). Multidimensional director modeling using the Q tensor representation in a liquid crystal cell and its application to the π cell with patterned electrodes. *Jpn. J. Appl. Phys.*, *38*, 135–146.
[8] Kreyszig, E. (1983). *Advanced Engineering Mathematics*. John Wiley & Sons: New York.
[9] Nose, T., Honma, M., & Sato, S. (2000). Influence of the spherical substrate in the liquid crystal lens on the optical properties and molecular orientation state. *Proc. SPIE.*, *4418*, 120–128.